The trapping in high-shear regions of slender bacteria undergoing chemotaxis in a channel

R. N. Bearon[1]† and A. L. Hazel[2]

[1] Department of Mathematical Sciences, University of Liverpool, Liverpool, L69 7ZL, UK
[2] School of Mathematics, University of Manchester, Manchester M13 9PL, UK

(Received ?; revised ?; accepted ?. - To be entered by editorial office)

Recently published experimental observations of slender bacteria swimming in channel flow demonstrate that the bacteria become trapped in regions of high shear, leading to reduced concentrations near the channel's centreline. However, the commonly-used, advection-diffusion equation, formulated in macroscopic space variables and originally derived for unbounded homogeneous shear flow, predicts that the bacteria concentration is uniform across the channel in the absence of chemotactic bias. In this paper, we instead use a Smoluchowski equation to describe the probability distribution of the bacteria, in macroscopic (physical) and microscopic (orientation) space variables. We demonstrate that the Smoluchowski equation is able to predict the trapping phenomena and compare the full numerical solution of the Smoluchowski equation with the experimental results when there is no chemotactic bias and also in the presence of a uniform cross-channel chemotactic gradient. Moreover, a simple analytic approximation for the equilibrium distribution provides an excellent approximate solution for slender bacteria, suggesting that the dominant effect on equilibrium behaviour is flow-induced modification of the bacteria's swimming direction. A continuum framework is thus provided to explain how the equilibrium distribution of slender chemotactic bacteria is altered in the presence of spatially varying shear flow. In particular we demonstrate that whilst advection is an appropriate description of transport due to the mean swimming velocity, the random re-orientation mechanism of the bacteria cannot be simply modelled as diffusion in physical space.

Key words:

1. Introduction

Many bacteria are motile and inhabit a variety of dynamic fluid environments: from turbulent oceans to medical devices. Bacteria can bias their swimming in the presence of chemical cues, a process known as chemotaxis, which allows them to move towards preferable environments and away from harmful chemicals. Recent micro-fluidic experiments have uncovered new mechanisms by which fluid shear affects the spatial distribution of bacteria. Here we develop and analyse a mathematical model to explain observations of Rusconi *et al.* (2014) demonstrating the trapping of slender bacteria in regions of high shear in channel flow.

There has been much progress in modelling the collective dynamics of suspensions of swimming micro-organisms, including understanding phenomena such as gyrotaxis and

† Email address for correspondence: rbearon@liv.ac.uk

bioconvection (Pedley & Kessler 1992). A commonly used continuum description for micro-organism (cell) concentration is an advection-diffusion model in physical space, where directional swimming, for example chemotaxis, is captured by an advection term, and diffusion describes the random movements. As a first approximation, advection by the fluid can be simply added to this equation, an approach taken by Taylor & Stocker (2012) to model bacterial chemotaxis in turbulence. A more accurate approach, developed in the context of gyrotactic microorganisms, is to allow the directional swimming and diffusion coefficients to be modified by the flow (Pedley & Kessler 1990). Much recent interest has focussed on instabilities driven by the active swimming forces exerted on the fluid, again often using advection-diffusion models for cell concentration (Pedley 2010). In this paper we shall demonstrate that whilst advection is an appropriate description of transport due to the combination of fluid advection and mean swimming velocity, modelling the random movements by diffusion in physical space fails to capture the phenomenon of trapping in high shear.

An alternative continuum approach is to consider a Smoluchowski equation describing evolution of the distribution of cells in physical and orientation space, as reviewed by Saintillan & Shelley (2013). For unbounded homogeneous shear flow, using the theory of Generalized Taylor Dispersion, the Smoluchowski equation has previously been shown, after sufficient time, to be approximated by an advection-diffusion equation in physical space only (Frankel & Brenner 1993; Manela & Frankel 2003). However, this approach can fail for inhomogeneous shear flow and we have previously shown that the full Smoluchowski equation can be useful in identifying the true distribution (Bearon *et al.* 2011). In this paper we demonstrate that by deriving the equilibrium solution of the Smoluchowski equation we can replicate the experimental observation of trapping in high shear.

The overall aim of this paper is to develop a mathematical formalism to describe populations of slender chemotactic bacteria in shear. We begin in §2 by introducing the governing Smoluchowski equation appropriate for a flow field that advects and rotates elongated axisymmetric cells and assume the cells undertake run-and-tumble chemotaxis. In addition, the cells experience translational and rotational diffusion. After explaining why an advection-diffusion equation in physical space cannot capture experimental observations, we restrict attention to a simplified two-dimensional geometry in which the flow field is parabolic and the chemoattractant gradient is constant and perpendicular to the flow direction. In section 3, results are presented for the equilibrium distribution of cells across the channel for a range of values of Pe, the flow Péclet number, for both non-chemotactic and chemotactic cells. The distributions are computed using the numerical solution of Smoluchowski equation by finite elements, and also from an analytic approximation obtained via an asymptotic expansion for small ϵ, the swimming Péclet number. The results are compared with experimental data, and the mechanism for trapping explained. We draw our conclusions in section 4.

2. Model

2.1. *Conservation equation for* $\psi(\boldsymbol{x}, \boldsymbol{p}, t)$

Our starting point is a conservation equation for the probability distribution function $\psi(\boldsymbol{x}, \boldsymbol{p}, t)$ representing the distribution of swimmer position $\boldsymbol{x}$ and orientation $\boldsymbol{p}$ at time t as reviewed by Saintillan & Shelley (2013):

$$\frac{\partial \psi}{\partial t} + \boldsymbol{\nabla}_{\boldsymbol{x}} \cdot (\dot{\boldsymbol{x}}\psi) + \boldsymbol{\nabla}_{\boldsymbol{p}} \cdot (\dot{\boldsymbol{p}}\psi)$$

$$+\lambda(\boldsymbol{x},\boldsymbol{p},t)\psi - \int_\Omega \lambda(\boldsymbol{x},\boldsymbol{p}',t)K(\boldsymbol{p},\boldsymbol{p}')\psi(\boldsymbol{x},\boldsymbol{p}',t)d\boldsymbol{p}' = 0, \tag{2.1}$$

where $\boldsymbol{\nabla}_{\boldsymbol{p}}$ denotes the gradient operator on the unit sphere of orientations Ω. The first line accounts for changes due to the translational flux velocity, $\dot{\boldsymbol{x}}$, and orientational flux velocity, $\dot{\boldsymbol{p}}$, which are given by, again see Saintillan & Shelley (2013),

$$\dot{\boldsymbol{x}} = \boldsymbol{u} + V_s\boldsymbol{p} - D\boldsymbol{\nabla}_{\boldsymbol{x}}\ln\psi, \tag{2.2}$$

$$\dot{\boldsymbol{p}} = \beta\boldsymbol{p}\cdot\mathsf{E}\cdot(\mathsf{I}-\boldsymbol{pp}) + \frac{1}{2}\boldsymbol{\omega}\wedge\boldsymbol{p} - d_r\boldsymbol{\nabla}_{\boldsymbol{p}}\ln\psi. \tag{2.3}$$

The translational flux velocity of the cell is a combination of fluid velocity, $\boldsymbol{u}$, cell swimming velocity, $V_s\boldsymbol{p}$, and translational Brownian diffusion, D. The orientational flux velocity represents an axisymmetric cell (with shape factor β) rotated by viscous forces in a flow characterised by the rate-of-strain tensor E and vorticity vector $\boldsymbol{\omega}$. We also include rotational diffusion of magnitude d_r, which may model intrinsic cell behaviour in addition to Brownian rotational diffusion. The shape factor, $0 \leqslant \beta \leqslant 1$, characterises the slenderness of the cell; and $\beta = 0$ for a sphere.

The first term on the second line of equation (2.1) models bacteria that tumble away from orientation $\boldsymbol{p}$ with frequency $\lambda(\boldsymbol{x},\boldsymbol{p},t)$ and the second term represents bacteria that tumble from orientation $\boldsymbol{p}'$ with frequency $\lambda(\boldsymbol{x},\boldsymbol{p}',t)$ and choose a new orientation $\boldsymbol{p}$ with probability $K(\boldsymbol{p},\boldsymbol{p}')$. We note that $\int_\Omega K(\boldsymbol{p},\boldsymbol{p}')d\boldsymbol{p} = 1$. For run-and-tumble chemotaxis, the frequency of tumbles depends on the change in chemical concentration experienced by the cell. For linear (weak) chemotactic response, assuming the chemical gradient is steady, homogeneous and perpendicular to the fluid velocity, we obtain a simple expression for the tumble rate, used previously for example by Bearon & Pedley (2000):

$$\lambda(\boldsymbol{p}) = \lambda_0(1 - \zeta V_s\boldsymbol{p}\cdot\boldsymbol{\nabla}s), \tag{2.4}$$

where λ_0 is the tumble rate in the absence of chemical gradient, ζ is the chemotactic response strength and s is the chemoattractant concentration.

2.2. *Boundary condition*

Integrating equation (2.1) over all orientations yields a conservation equation for the cell concentration, $n(\boldsymbol{x},t) = \int_\Omega \psi(\boldsymbol{x},\boldsymbol{p},t)d\boldsymbol{p}$:

$$\frac{\partial n}{\partial t} + \boldsymbol{\nabla}_{\boldsymbol{x}}\cdot\boldsymbol{J} = 0, \tag{2.5}$$

where the cell flux, $\boldsymbol{J}$ is given by:

$$\boldsymbol{J} = \int_\Omega \left((\boldsymbol{u} + V_s\boldsymbol{p})\psi - D\boldsymbol{\nabla}_{\boldsymbol{x}}\psi\right)\, d\boldsymbol{p}. \tag{2.6}$$

In confined geometries, e.g. within a channel, to impose zero cell flux through the walls, specified by the normal vector $\hat{\boldsymbol{n}}$, we require that $\boldsymbol{J}\cdot\hat{\boldsymbol{n}} = 0$. Assuming standard no slip boundary conditions for the fluid and impermeable walls, the normal component of fluid velocity is zero at the walls. Thus, the no flux condition is given by

$$\left(\int_\Omega V_s\boldsymbol{p}\psi d\boldsymbol{p} - D\boldsymbol{\nabla}_{\boldsymbol{x}}n\right)\cdot\hat{\boldsymbol{n}} = 0. \tag{2.7}$$

2.3. *Population-level model*

In previous work on Generalized Taylor Dispersion (Manela & Frankel (2003); Bearon (2003)), it has been shown that on timescales long compared to the random reorientation

timescales, $1/d_r$ or $1/\lambda_0$, the cell concentration in unbounded homogeneous shear flow with uniform chemical gradient satisfies an advection-diffusion equation in physical space:

$$\frac{\partial n}{\partial t} + \boldsymbol{\nabla}_{\boldsymbol{x}} \cdot [(\boldsymbol{u} + V_s \boldsymbol{q})\, n - \mathsf{D} \cdot \boldsymbol{\nabla}_{\boldsymbol{x}} n] = 0, \tag{2.8}$$

where $\boldsymbol{q}$ is the mean swimming direction and D is the diffusion tensor which represents the random components of swimming in addition to translational Brownian diffusion. Whilst the diffusion tensor takes quite a complex form, the mean swimming direction is given by $\boldsymbol{q} = \int_\Omega \boldsymbol{p} f(\boldsymbol{p}) d\boldsymbol{p}$, where $f(\boldsymbol{p})$ is the equilibrium orientation distribution, which satisfies

$$\boldsymbol{\nabla}_{\boldsymbol{p}} \cdot (\dot{\boldsymbol{p}} f) + \lambda(\boldsymbol{p}) f - \int_\Omega \lambda(\boldsymbol{p}') K(\boldsymbol{p}, \boldsymbol{p}') f d\boldsymbol{p} = 0. \tag{2.9}$$

We note that for unbounded homogeneous shear flow and uniform chemical gradient, the equilibrium orientation distribution is independent of spatial position, that is the function $f(\boldsymbol{p})$ is independent of $\boldsymbol{x}$.

2.4. *Two-dimensional channel flow*

Motivated by recent micro-fluidic experiments (Rusconi *et al.* 2014), we consider parabolic planar flow through a channel of width W:

$$\boldsymbol{u} = U \left(1 - 4 \left(\frac{Y}{W}\right)^2\right) \boldsymbol{i}, \tag{2.10}$$

where U is the flow velocity at the centreline of the channel. We choose plane Cartesian coordinates (X, Y), with respective base vectors $(\boldsymbol{i}, \boldsymbol{j})$, such that the walls of the channel are located at $Y = \pm W/2$. Although we are now considering variable shear flow in a confined region, it is common to assume that the population of cells can still be approximated by an advection-diffusion equation of the form given by equation (2.8), provided that the flow-induced reorientation of the cells is sufficiently fast. If we impose zero cell flux at the wall, the equilibrium distribution for the cell concentration is then given by

$$n(Y) = n(0) \exp\left(\int_0^Y \frac{V_s q_Y}{D_{YY}} dY\right). \tag{2.11}$$

For unbiased swimmers, we expect the mean vertical swimming speed, $V_s q_Y$, to be zero and we thus predict a uniform distribution for cells at equilibrium. However this contradicts observed depletion of bacteria in the central regions of a channel in the absence of chemical gradients (Rusconi *et al.* 2014).

In order to simplify subsequent numerical and analytic investigation, we now restrict attention to the mathematically simpler case of cells constrained to a two-dimensional plane, and so define the swimming direction vector in terms of the angle θ:

$$\boldsymbol{p} = \cos\theta \boldsymbol{i} + \sin\theta \boldsymbol{j}. \tag{2.12}$$

We non-dimensionalise such that $(x, y) = (2X/W, 2Y/W)$ and the channel walls are at $y = \pm 1$. We take the chemoattractant gradient to be in the positive cross-channel (y) direction and independent of x, and take the tumble rate to decrease linearly with chemotactic gradient, equation (2.4). Also for mathematical simplicity we shall focus attention on isotropic tumbles, taking

$$K(\theta, \theta') = \frac{1}{2\pi}. \tag{2.13}$$

Swimming speed	V_s	$50\mu\text{ms}^{-1}$	
Rotational diffusion	d_r	1s^{-1}	
Tumble rate	λ_0	2s^{-1}	
Channel width	W	$425\mu m$	
Brownian translation diffusion[1]	D	$2\times10^{-9}\text{cm}^2\text{s}^{-1}$	Berg (1993)
Cell shape factor	β	0.99	
Chemotactic strength	χ	0.99	Fit to data
Flow Péclet number	$Pe = 2U/Wd_r$	0-50	
Swimming Péclet number	$\epsilon = 2V_s/Wd_r$	0.2	
Relative tumble rate	$\sigma = \lambda_0/d_r$	2	
Relative translation diffusion	$d = Dd_r/V_s^2$	10^{-4}	
Cartesian co-ordinates	(X, Y)		
Dimensionless co-ordinates	$(x, y) = (2X/W, 2Y/W)$		

TABLE 1. Default parameter values, obtained from Rusconi *et al.* (2014) unless stated otherwise. [1] For a sphere of radius $a = 10^{-4}$cm in water at room temperature.

Non-dimensionalising time on d_r, from the governing equations (2.1-2.3), we obtain an equation for the equilibrium distribution $\psi(y,\theta)$:

$$\epsilon\frac{\partial}{\partial y}(\sin\theta\psi) - \epsilon^2 d\frac{\partial^2\psi}{\partial y^2} + \frac{\partial}{\partial\theta}\left(yPe(1-\beta\cos2\theta)\psi - \frac{\partial\psi}{\partial\theta}\right) + (\sigma - \epsilon\chi\sin\theta)\psi - \frac{1}{2\pi}\int_0^{2\pi}(\sigma-\epsilon\chi\sin\theta')\psi(y,\theta')d\theta' = 0, \tag{2.14}$$

where the non-dimensional parameters governing the system are given as follows: $\epsilon = 2V_s/Wd_r$ is the swimming Péclet number; $Pe = 2U/Wd_r$ is the flow Péclet number; $d = Dd_r/V_s^2$ is the ratio of Brownian diffusion to diffusion generated by random swimming; $\sigma = \lambda_0/d_r$ is the ratio of tumble rate to rotational diffusion rate; and $\chi = \lambda_0\zeta\frac{ds}{dy}$ measures the chemotactic strength. The concentration is subject to a normalisation condition $\int_{-1}^{1}\int_{\theta=0}^{2\pi}\psi(y,\theta)d\theta dy = 1$ and the zero flux boundary condition on the walls (equation 2.7) can be expressed as

$$\int_0^{2\pi}\left(\sin\theta\psi - \epsilon d\frac{\partial\psi}{\partial y}\right)d\theta\Big|_{y=\pm1} = 0. \tag{2.15}$$

Parameter estimates are detailed in table 1.

3. Results & discussion

3.1. *Numerical results*

The full equation for ψ, equation (2.14), is solved numerically using a Galerkin finite element method. Equation (2.14) is converted into a weak form on multiplication by a test function $N(y,\theta)$, integrating over the finite domain and then integrating by parts:

$$\int_0^{2\pi}\int_{-1}^{1}\epsilon\left[\sin\theta\psi - \epsilon d\frac{\partial\psi}{\partial y}\right]\frac{\partial N}{\partial y} + \left[yPe(1-\beta\cos2\theta)\psi - \frac{\partial\psi}{\partial\theta}\right]\frac{\partial N}{\partial\theta}\,\mathrm{d}y\,\mathrm{d}\theta + \int_0^{2\pi}\int_{-1}^{1}\left[(\epsilon\chi\sin\theta - \sigma)\psi + I\right]N\,\mathrm{d}y\,\mathrm{d}\theta = 0, \tag{3.1}$$

where $I(y)$, the integral term, is treated as a new variable approximated by Galerkin projection in the y direction

$$\int_{-1}^{1}\left[\frac{1}{2\pi}\int_{0}^{2\pi}(\sigma-\epsilon\chi\sin\theta')\psi(y,\theta')d\theta'-I\right]\overline{N}(y)\mathrm{d}y=0. \tag{3.2}$$

$\overline{N}$ represents the test functions restricted to the y-direction by integration over θ. Periodic boundary conditions are applied in the θ direction and the omission of boundary terms arising from integration by parts enforces the natural boundary condition of no vertical flux $\sin\theta\psi-\epsilon d\frac{\partial\psi}{\partial y}=0$, pointwise on the walls $y=\pm1$. Note that this is a stronger condition than the integral condition (2.15), but it is required to prevent the appearance of eigenfunctions in the solution that lead to non-uniqueness (see supplementary material). The normalisation condition is enforced by fixing ψ at a single node and then renormalising once the solution has been obtained. The equations are discretised using standard quadratic finite elements on a grid of $100(\theta)\times500(y)$. The elements are uniformly spaced in the θ direction, but high resolution and non-uniform spacing in the y direction are required to accurately resolve thin diffusion boundary layers near the walls. A piecewise linear scaling is applied such that half the elements are contained within the regions $|y|\geqslant0.98$. The discrete system of equations was assembled and solved using the C++ library `oomph-lib` (Heil & Hazel 2006).

Figure 1 shows the equilibrium cell concentration, $n(y)=\int_0^{2\pi}\psi(y,\theta)d\theta$, in the absence of chemical gradient. We find that a significant number of cells are contained within the boundary-layers that arise from the boundary conditions imposed in the numerical simulations, which explains the discrepancy between the simulations and asymptotic approximations even at $Pe=0$. As the flow strength, as measured by Pe, increases, cells are depleted in the central low-shear regions of the channel and accumulate in the high-shear regions near the boundaries. The numerical solution under-estimates the accumulation of cells at the boundaries. This could be due to the neglect of various mechanisms, including hydrodynamic interactions with the walls, which have previously been shown to generate boundary accumulations, as reviewed by Lauga & Powers (2009). We also see that tumbling reduces the amount of depletion in both numerical simulation and experiments. However, we note that the estimate we take for rotational diffusion, d_r, is that given by Rusconi *et al.* (2014) which incorporated all random reorientation mechanisms including tumbling. Therefore the most appropriate comparison for experimental data on tumbling cells is actually the numerical simulation with $\sigma=0$.

In figure 1, which is for very slender cells corresponding to $\beta=0.99$, the numerical solution under-estimates the depletion at intermediate Pe and we find that the central depletion increases monotonically with shear rate, unlike the experimental findings of Rusconi *et al.* (2014). These latter observations are consistent with the Fokker–Planck solutions of Rusconi *et al.* (2014), which bear resemblance to the small ϵ asymptotic solutions in the next section.

Figure 2 shows the dependence of the cell concentration on the shape parameter β. For spherical cells, $\beta=0$, the cell concentration is uniform throughout the channel. For moderate Pe, from 1.25 to 10, the cell concentration shows monontonic depletion at the centre of the channel with increasing values of β. At $Pe=25$, the numerical solution disagrees with the small ϵ asymptotic solution and exhibits non-montonic changes in centreline concentration, as well as symmetric peaks in cell concentration away from the walls which increase in amplitude at small β and then decay at larger β. We note Rusconi *et al.* (2014) observed similar double peaks away from the centreline in simulations where random reorientation mechanisms were neglected. At sufficiently high Pe, the balance

between vertical and rotational advection occurs at a larger lengthscale $y \sim \epsilon^{1/2} Pe^{-1/2}$ than the balance between rotational diffusion and advection $y \sim Pe^{-1}$. Thus, the dominant balance in the small ϵ asymptotics is incorrect and the random reorientation only operates in an inner region near $y = 0$. Furthermore, the experimental findings of Rusconi *et al.* (2014) showing that the central depletion increases non-monotonically with shear rate are consistent with our model if the experimental estimate of $\beta = 0.99$ is an overestimate. For slightly smaller values of β, the central depletion changes non-monotonically with Pe, see Figure 2(f). O'Malley & Bees (2012) have shown that the effective cell eccentricity of a swimming cell is much smaller than for the inanimate body alone, giving credence to the claim that $\beta = 0.99$ may be an over-estimate.

Figure 3 shows the corresponding equilibrium cell concentration for chemotactic cells. In the absence of shear, cells move up the chemical gradient and at equilibrium, the balance between chemotactic drift up the chemical gradient and diffusion down the cell concentration gradient yields an exponential distribution in cell concentration. We see that the fitted distribution corresponds to $\chi \approx 1$, which is to be expected as the chemical gradient in the experiment was such that the effect of chemotaxis was visible throughout the channel in still fluid. By introducing non-uniform shear through the channel, this equilibrium distribution is modified. As for the non-tumbling cells, there is a depletion of cells in the central low-shear regions of the channel. In the numerical simulations, the tumble rate, σ, is non-zero in order to model run-and-tumble chemotaxis. As the estimate for rotational diffusion, d_r, given by Rusconi *et al.* (2014) incorporates reorientation due to tumbles, in the numerical simulations with non-zero σ the rotational diffusion is overestimated.

3.2. *Equilibrium cell concentration via small ϵ asymptotics*

To understand the mechanism for cell depletion in low shear, we consider a perturbation solution for $\epsilon \ll 1$, and neglect Brownian translation diffusion, $d = 0$. Specifically we consider a pertubation expansion for ψ:

$$\psi = n(y) f^{(0)}(\theta; y) + \epsilon \psi^{(1)}(y, \theta), \tag{3.3}$$

where $\int_0^{2\pi} f^{(0)}(\theta; y) d\theta = 1$, and $f^{(0)}$ is periodic in θ. On inserting this expression into equation (2.14), we obtain at leading order in ϵ

$$\frac{\partial}{\partial \theta}\left(yPe(1 - \beta \cos 2\theta) f^{(0)} - \frac{\partial f^{(0)}}{\partial \theta} \right) + \sigma(f^{(0)} - \frac{1}{2\pi}) = 0, \tag{3.4}$$

the solution of which is found numerically (see supplementary material). We can interpret $f^{(0)}(\theta; y)$ as the leading-order equilibrium orientation distribution at a given cross-channel position y.

On integrating equation (2.14) from $\theta = 0$ to 2π and noting that ψ is periodic in θ we obtain at leading order in ϵ

$$\frac{d}{dy}\left(\int_0^{2\pi} \sin\theta \psi^{(1)} d\theta \right) = 0.$$

Imposing the zero flux boundary condition on the walls $y = \pm 1$ we obtain the zero flux condition:

$$\int_0^{2\pi} \sin\theta \psi^{(1)} d\theta = 0. \tag{3.5}$$

Multiplying equation (2.14) by $\sin\theta$, integrating over θ, and applying the zero flux

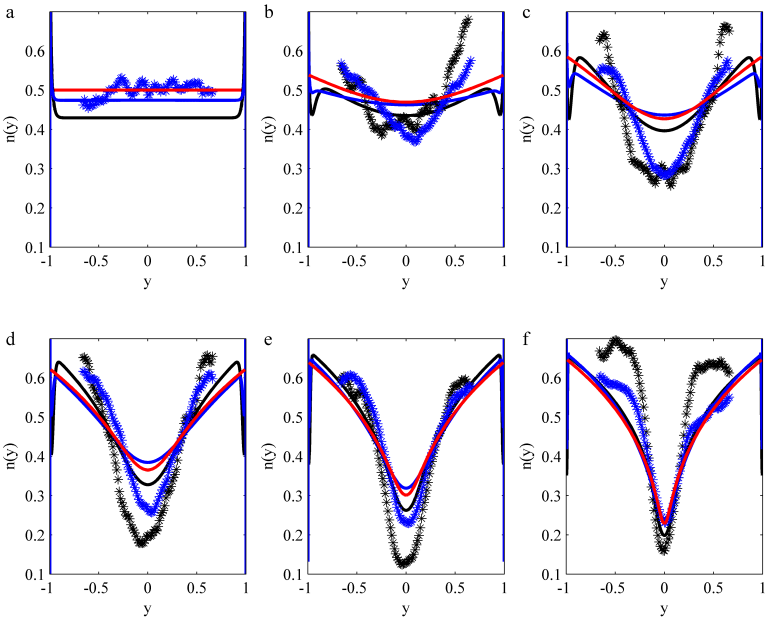

FIGURE 1. Equilibrium cell concentration across the channel in the absence of a chemotactic gradient, $\chi = 0$. Black line, numerical solution of ψ equation with non-tumbling cells $\sigma = 0$; Blue line, numerical solution of ψ equation with tumbling cells $\sigma = 2$; Red line, leading order in ϵ asymptotic approximation with non-tumbling cells $\sigma = 0$; Black stars, experiments on smooth-swimming cells; Blue stars, experiments on tumbling cells. $Pe = [0, 1.25, 2.5, 5, 10, 25]$ corresponds to (a-f) respectively.

condition (3.5), yields at $O(\epsilon)$

$$\frac{d}{dy}\left(nV_{MS}\right) - \chi n V_{MS} - yPe \int_0^{2\pi} \cos\theta(1 - \beta\cos 2\theta)\psi^{(1)} d\theta = 0, \tag{3.6}$$

where

$$V_{MS}(y) = \int_0^{2\pi} \sin^2\theta f^{(0)}(\theta; y) d\theta \tag{3.7}$$

is the mean squared vertical swimming speed at a given position, y.

If we choose to neglect the $O(\epsilon)$ perturbation to ψ, that is set $\psi^{(1)} = 0$, we obtain an expression for the equilibrium cell concentration:

$$n(y) = n(0)V_{MS}(0)\frac{e^{\chi y}}{V_{MS}(y)}. \tag{3.8}$$

In figure 1, the leading-order approximation in the absence of chemical gradient is shown to agree well with the full numerical solution for a wide range of Pe. To explain the phenomenon of trapping in high shear, we see from figure 4 that the straining motion causes the orientation distribution of slender cells to deviate from uniform, and become increasingly peaked towards the horizontal. We note that individual cells do not maintain an orientation aligned with the horizontal, rather they undergo noisy Jeffery orbits with a determinstic, orientation-dependent angular velocity resulting in a non-uniform orientation distribution (Guazzelli & Morris 2012). This peak in orientation distribu-

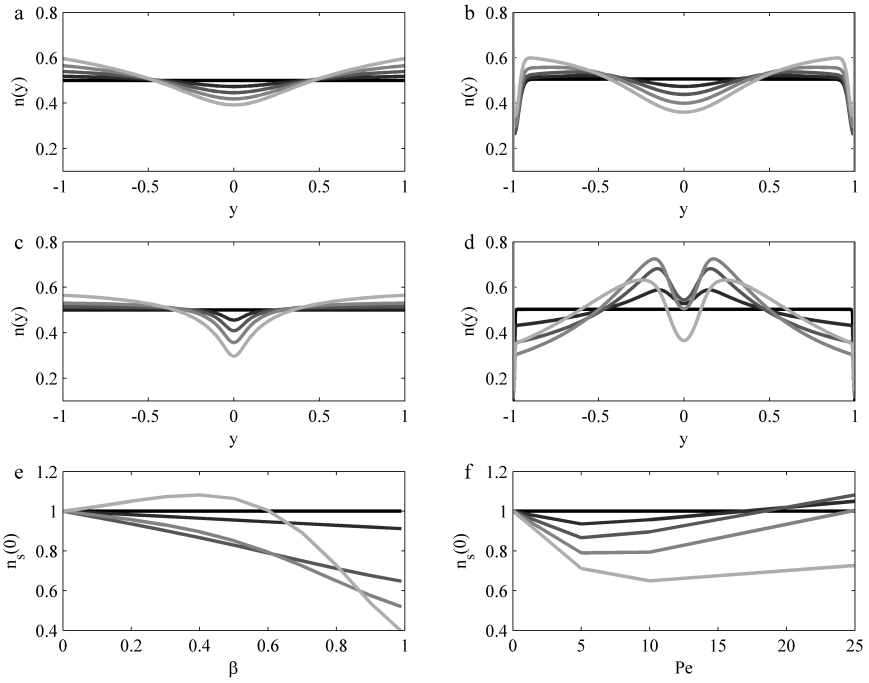

FIGURE 2. The influence of cell shape, β, on equilibrium cell concentration with $\chi = \sigma = 0$. (a,b) correspond to $Pe = 5$ and (c,d) to $Pe = 25$. (a,c) Leading order in ϵ asymptotic approximation, other plots correspond to numerical solution of ψ equation. In (e,f) $n_s(0)$ is the cell concentration at $y = 0$ normalised by the $\beta = 0$ solution at the corresponding Pe. In (a-d,f) greyscale indicate $\beta = [0, 0.2, 0.4, 0.6, 0.8]$ with black corresponding to 0; in (e) greyscale indicate $Pe = [0, 1.25, 5, 10, 25]$ with black corresponding to 0.

tion towards the horizontal reduces the mean squared vertical speed, V_{MS} and generates accumulation of cells in regions of high shear. This mechanism for accumulation via a reduction in effective vertical speed was predicted by Rusconi *et al.* (2014). However the details of their calculation were different to our current work and did not include chemotaxis. Specifically, they predicted that the concentration profile of cells should be inversely proportional to the average vertical component of upwards swimming cells, $\int_0^\pi \sin\theta f^{(0)}(\theta; y) d\theta$. They used a Fokker-Plank description for the orientation distribution at a given vertical position, equivalent to equation (3.4) with $\sigma = 0$. However to derive the resultant cell concentration, they adapted a one-dimensional random walk model instead of analyzing the space-orientation distribution.

The agreement between the asymptotic approximation and full numerical solution is not good at small β and large values of Pe, see Figure 2, because the dominant balance between rotational advection and diffusion is no longer appropriate and the vertical advection term must be included at leading order. As β increases, the effective Pe decreases because most cells are concentrated near $\theta = 0$ and π and the dominant balance required in the asymptotics is regained.

For slender chemotactic cells, there is good agreement between the analytic approximation and the full numerical solution as shown for a range of Pe in figure 3. We should note that the profile is dominated by the exponential in chemotactic strength parameter,

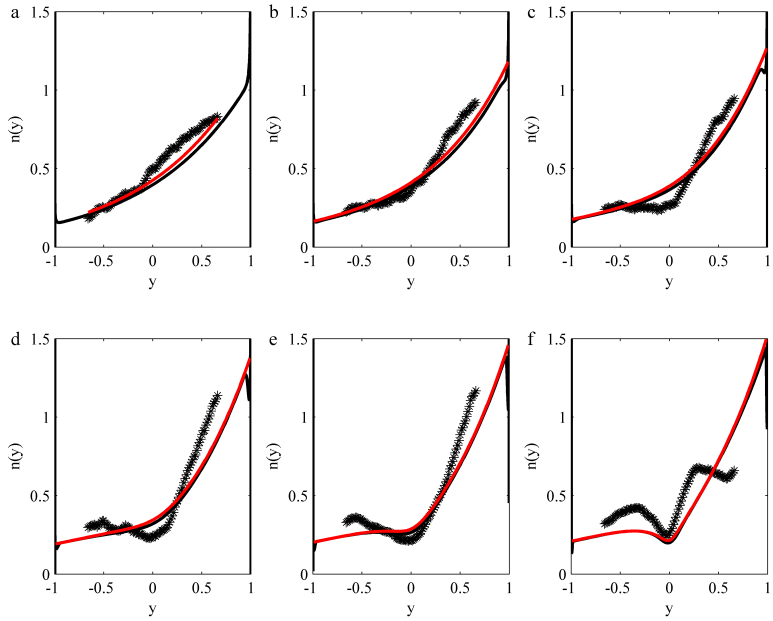

FIGURE 3. Equilibrium concentration with cross-channel chemotactic gradient. Black line, numerical solution of ψ equation; Red line, leading order in ϵ asymptotic approximation; Black stars, experiments. $Pe = [0, 1.25, 2.5, 5, 10, 25]$ corresponds to (a-f) respectively. Parameters: $\chi = 0.99$ (fit using $Pe = 0$ experimental data); $\sigma = 2$.

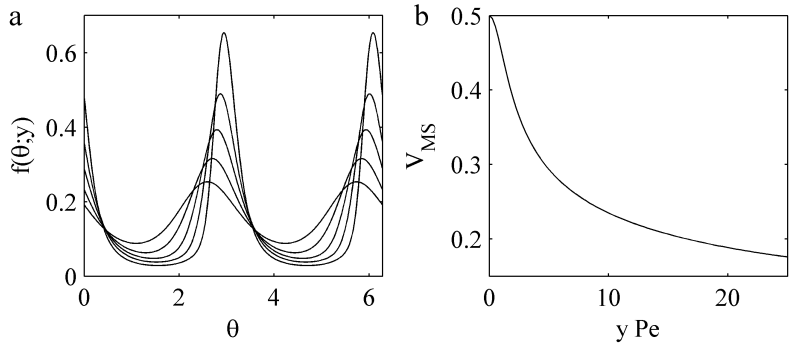

FIGURE 4. Non-tumbling cells, $\sigma = \chi = 0$. (a) Equilibrium orientation distribution, $f^{(0)}(\theta; y)$, for values of $yPe = [1.25, 2.5, 5, 10, 25]$. As the shear increases, the orientation distribution is increasingly peaked around the horizontal, $\theta = 0, \pi$. (b) The mean squared vertical swimming speed, V_{MS} as a function of the local shear strength, yPe.

χ which was obtained via a nonlinear fit of equation (3.8) to the experimental data in the absence of shear to obtain $\chi = 0.99$. Thus, the good agreement between experiments and numerical solution at $Pe = 0$ is a consequence of this fitting. Note that non-monotonic centreline depletion with increasing Pe still occurs at smaller values of β for chemotactic cells (see supplementary material).

For $Pe \ll 1$, we can obtain $f^{(0)}$ correct to $O(Pe^2)$ (as computed by Rusconi *et al.* (2014) for $\sigma = 0$, also see supplementary material) and thus obtain from equation (3.8),

an approximate expression for the equilibrium distribution:

$$n(y) = n(0)\left(1 + \frac{\beta y^2 Pe^2}{8(1+\sigma/4)^2}\right)e^{\chi y}. \tag{3.9}$$

We see that, in this limit, accumulation is proportional to the shape factor, β and scales as Pe^2. Furthermore, we note that tumbling, as measured by σ, increases the amount of reorientation experienced by cells. Thus in regions of high shear, the non-uniformity of $f^{(0)}$ is reduced causing an increase in V_{MS}. This results in a reduction in the amount of cell aggregation in high shear regions, as seen on comparing the tumbling and non-tumbling data and numerical solution in figure 1.

4. Conclusions

We have developed a continuum framework to describe the spatial distribution of slender chemotactic bacteria in channel flow which captures recently published experimental observations. In addition to solving the cell conservation equation numerically, we have obtained a simple analytic expression for the equilibrium distribution which helps understand the mechanism by which the distribution of cells is modified by fluid shear. The analytic expression is in good agreement with the numerical solutions for all cell shapes (β) at moderate shear rates (Pe), but is only appropriate at higher Pe for very slender cells for which the rotational diffusion is of a similar magnitude to flow-induced reorientation. This work contributes to the understanding of hydrodynamic phenomena in suspensions of active swimmers, in particular it highlights potential problems in modelling the random reorientation mechanism of bacteria in inhomogeneous shear as diffusion in physical space, and demonstrates the utility of an alternative framework, that of the Smoluchowski equation, which is still compatible with classical models of Stokesian swimmers.

For slender cells, when compared to the experimental data, the gradients in concentration are underestimated by the Smoluchowski equation, leading to underprediction of the depletion zone. On increasing Pe the model predictions of centreline depletion move closer to the experimental data, unlike the individual-based simulations of Rusconi *et al.* (2014) which overpredict depletion for high Pe. In contrast to the experimental results, the depletion increases monotonically with Pe for the slender cells ($\beta = 0.99$), but our model predicts non-monotonic behaviour for slightly less slender cells, which may suggest that the effective cell shape factor is smaller than previously estimated. Furthermore, when solving the Smoluchowski equation numerically, we identified that an important area for future study is the boundary condition at the wall, which can have a dramatic effect on the global concentration field.

Many refinements are possible to this model framework in order to improve the agreement with experimental data. We have considered cells constrained to move in a two-dimensional plane and we note that care must be applied in extending the results to cells free to move in three-dimensions. Throughout this work we have neglected feedback that swimming has on the flow field, yet even at low volume fractions, hydrodynamic interactions between cells and with boundaries can be important, for example leading to bioconvection and boundary accumulations respectively. At high volume fractions, the swimming stresses exerted on the fluid can drive fluid motions on spatial and temporal scales much larger than the individual cells (Lushi *et al.* 2012). We have considered a very simple description of chemotaxis, which could be modified to take account of the observation that shear flow has been shown to significantly impact how cells temporally integrate the chemical signal (Locsei & Pedley 2009). Furthermore bacteria display a

range of behaviours, and optimal swimming strategy can depend on the fluid dynamics (Stocker 2011).

The results presented here may be relevant not only to bacteria in pipe flow, but to unbounded flow such as in the turbulent ocean. Whilst previous work has demonstrated bacterial accumulation at surfaces due to hydrodynamic interactions, reviewed by Lauga & Powers (2009), the phenomenon of trapping in high shear discussed here is not restricted to boundary accumulation but may also be relevant to high-shear interior regions.

R. Rusconi and R. Stocker provided experimental motivation for this work and generously discussed their data and analysis.

REFERENCES

Bearon, R. N. 2003 An extension of generalized Taylor dispersion in unbounded homogeneous shear flows to run-and-tumble chemotactic bacteria. *Phys. Fluids* **15** (6), 1552 – 1563.

Bearon, R. N., Hazel, A. L. & Thorn, G. J. 2011 The spatial distribution of gyrotactic swimming micro-organisms in laminar flow fields. *J. Fluid Mech.* **680**, 602–635.

Bearon, R. N. & Pedley, T. J. 2000 Modelling run-and-tumble chemotaxis in a shear flow. *Bull. Math. Biol.* **62** (4), 775 – 791.

Berg, H. C. 1993 *Random walks in biology*. Princeton University Press.

Frankel, I. & Brenner, H. 1993 Taylor dispersion of orientable Brownian particles in unbounded homogeneous shear flows. *J. Fluid. Mech.* **255**, 129 – 156.

Guazzelli, E & Morris, J. F. 2012 *A Physical Introduction to Suspension Dynamics*. Cambridge University Press.

Heil, M. & Hazel, A. L. 2006 `oomph-lib` — An object-oriented multi-physics finite-element library in fluid structure interaction. In *Lecture notes on computational science and engineering* (ed. M. Schafer & H.-J. Bungartz), pp. 19–49. Springer-Verlag.

Lauga, E. & Powers, T. R. 2009 The hydrodynamics of swimming microorganisms. *Rep. Prog. Phys.* **72**, 096601.

Locsei, J. T. & Pedley, T. J. 2009 Run and tumble chemotaxis in a shear flow: The effect of temporal comparisons, persistence, rotational diffusion, and cell shape. *Bull. Math. Biol.* **71**, 1089–1116.

Lushi, E., Goldstein, R. E. & Shelley, M. J. 2012 Collective chemotactic dynamics in the presence of self-generated fluid flows. *Phys. Rev. E* **86**, 040902.

Manela, A. & Frankel, I. 2003 Generalized Taylor dispersion in suspensions of gyrotactic swimming micro-organisms. *J. Fluid. Mech.* **490**, 99 – 127.

O'Malley, S. & Bees, M. A. 2012 The orientation of swimming biflagellates in shear flows. *Bull. Math. Biol.* **74**, 232–255.

Pedley, T. J. 2010 Instability of uniform micro-organism suspensions revisited. *J. Fluid Mech.* **647**, 335–359.

Pedley, T. J. & Kessler, J. O. 1990 A new continuum model for suspensions of gyrotactic microorganisms. *J. Fluid. Mech.* **212**, 155 – 182.

Pedley, T. J. & Kessler, J. O. 1992 Hydrodynamic phenomena in suspensions of swimming microorganisms. *Annu. Rev. Fluid Mech.* **24**, 313 – 358.

Rusconi, R., Guasto, J. S. & Stocker, R. 2014 Bacterial transport suppressed by fluid shear. *Nature Phys.* **10** (3), 212–217.

Saintillan, D. & Shelley, M. J. 2013 Active suspensions and their nonlinear models. *Comptes Rendus Physique* **14** (6), 497–517.

Stocker, R. 2011 Reverse and flick: Hybrid locomotion in bacteria. *Proc. Nat. Acad. Sci. USA* **108** (7), 2635–2636.

Taylor, J. R. & Stocker, R. 2012 Trade-offs of chemotactic foraging in turbulent water. *Science* **338** (6107), 675–679.